Acta Pharmaceutica Sinica B 2020;10(5):812–824

Chinese Pharmaceutical Association
Institute of Materia Medica, Chinese Academy of Medical Sciences

Acta Pharmaceutica Sinica B

www.elsevier.com/locate/apsb
www.sciencedirect.com

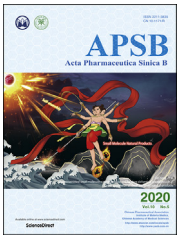

ORIGINAL ARTICLE

Berberine prevents primary peritoneal adhesion and adhesion reformation by directly inhibiting TIMP-1

Xin Liu[a,e,†], Yunwei Wei[b,†], Xue Bai[a,†], Mingqi Li[a], Huimin Li[a], Lei Wang[a], Shuqian Zhang[a], Xia Li[a], Tong Zhao[a], Yang Liu[b], Rui Geng[b], Hao Cui[a], Hui Chen[a], Ranchen Xu[a], Heng Liu[a], Yong Zhang[a,c,e,*], Baofeng Yang[a,d,e,*]

[a]*Department of Pharmacology (the State-Province Key Laboratories of Biomedicine-Pharmaceutics of China, Key Laboratory of Cardiovascular Research, Ministry of Education), College of Pharmacy, Harbin Medical University, Harbin 150081, China*
[b]*Department of Oncological and Laparoscopic Surgery, the First Affiliated Hospital of Harbin Medical University, Harbin 150001, China*
[c]*Institute of Metabolic Disease, Heilongjiang Academy of Medical Science, Harbin 150086, China*
[d]*Department of Pharmacology and Therapeutics, Melbourne School of Biomedical Sciences, Faculty of Medicine, Dentistry and HealthSciences University of Melbourne, Melbourne VIC 3010, Australia*
[e]*Research Unit of Noninfectious Chronic Diseases in Frigid Zone, Chinese Academy of Medical Sciences, 2019 Research Unit 070, Harbin 150081, China*

Received 20 September 2019; received in revised form 18 December 2019; accepted 15 January 2020

Abbreviations: ABSO, adhesive small bowel obstruction; BBR, berberine; ECM, extracellular matrix; EDC, 1-ethyl-3-(3-dimethylpropyl)-carbodiimide; FSP-1, fibroblasts specific protein 1; H&E, hemotoxylin and eosin; HPX, hemopexin-like; ICAM-1, intercellular cell adhesion molecule-1; LSPR, localized surface plasmon resonance; MMP-3, matrix metallopeptidase 3; MMP-8, matrix metallopeptidase 8; NHS, *N*-hydroxysuccinimide; NMR, nuclear magnetic resonance; PEG, polyethylene glycol; SPR, surface plasmon resonance; TIMP-1, tissue inhibitor of metalloproteinases 1; *Vegfα*, vascular endothelial growth factor α.

*Corresponding authors.
E-mail addresses: hmuzhangyong@hotmail.com (Yong Zhang), yangbf@ems.hrbmu.edu.cn (Baofeng Yang).

†These authors made equal contributions to this work.

Peer review under responsibility of Institute of Materia Medica, Chinese Academy of Medical Sciences and Chinese Pharmaceutical Association.

https://doi.org/10.1016/j.apsb.2020.02.003

KEYWORDS

Peritoneal adhesion;
Berberine;
Adhesion reformation;
TIMP-1

Abstract Peritoneal adhesions are fibrous tissues that tether organs to one another or to the peritoneal wall and represent the major cause of postsurgical morbidity. Enterolysis at repeat surgeries induces adhesion reformation that is more difficult to prevent than primary adhesion. Here we studied the preventive effects of different approaches of berberine treatment for primary adhesion, and its effects on adhesion reformation compared to Interceed. We found the primary adhesion was remarkably prevented by berberine through intraperitoneal injection 30 min before abrasive surgery (pre-berberine) or direct addition into injured cecum immediately after the surgery (inter-berberine). Rats with adhesion reformation had a more deteriorative collagen accumulation and tissue injury in abrasive sites than rats with primary adhesion. The dysregulated TIMP-1/MMP balance was observed in patients after surgery, as well as adhesion tissues from primary adhesion or adhesion reformation rats. Inter-berberine treatment had a better effect for adhesion reformation prevention than Interceed. Berberine promoted the activation of MMP-3 and MMP-8 by directly blocking TIMP-1 activation core, which was reversed by TIMP-1 overexpression in fibroblasts. In conclusion, this study suggests berberine as a reasonable approach for preventing primary adhesion formation and adhesion reformation.

1. Introduction

Intraperitoneal adhesions, a common post-abdominal operation long-term sequela, can develop in up to 94% of patients, increasing postoperative morbidity and causing adhesive small bowel obstruction (ASBO), chronic pelvic pain, and infertility[1,2]. Moreover, up to one-third of patients with intra-abdominal adhesions require a second operation for the release of existing adhesions, which can further increase the risk[3,4]. For patients admitted more than once for enterolysis, the relative risk of recurrent adhesion increases with increasing number of prior adhesion episodes, indicating the need for prevention of adhesion reformation. On the other hand, it is known that peritoneal injury due to surgery, infection or irritation begins before adhesion formation with fibrinous exudate and fibrin formation. Then fibroblasts invade the fibrin matrix with excessive collagen secretion and extracellular matrix (ECM) deposit followed by adhesion[5,6]. In normal healing process, ECM can be completely degraded by specific proenzyme matrix metalloprotease (MMP). However, if this process is inhibited by tissue inhibitors of MMPs (TIMP), peritoneal adhesions may be formed[7,8].

Several preventive agents against postoperative peritoneal adhesions have been investigated for their roles in activating fibrinolysis, hampering coagulation, diminishing the inflammatory response, inhibiting collagen synthesis, and creating a barrier between adjacent wound surfaces. However, these anti-adhesive agents were investigated primarily in animal models and have not been tested in patients, and they are mostly costly adding an enormous medical burden[9]. In addition, the reduction of adhesion reformation by these anti-adhesive agents appears to be less effective than the reduction of primary adhesion formation in both clinical practice and animal studies[7,8]. Undoubtedly, there is an urgent need for an effective formula for anti-adhesive therapy with minimal clinical disadvantages.

Berberine (BBR), the plant-derived isoquinoline alkaloid, has had a long history of application to the treatment of several conditions. It has multiple pharmaceutical formulations against cancer, obesity, diabetes, inflammation, atherosclerosis, hyperlipidemia and cardiovascular diseases[10]. Our previous study demonstrated that upon application to the abdominal cavity immediately after abrasive surgery, BBR effectively prevented intestinal adhesion through inhibition of intercellular cell adhesion molecule-1 (ICAM-1) secretion and expression downregulation of various inflammatory molecules[11]. However, it remained unstudied whether BBR could be used for preventing readily cicatricial adhesion reformation after enterolysis.

The aims of the present study were to compare the relative effectiveness of BBR with Interceed in preventing peritoneal adhesions and cicatricial adhesion reformation after enterolysis, and to decipher the underlying molecular mechanisms. For these purposes, both primary adhesion and enterolysis rat models were employed in our study, and isolated fibroblasts from adhesion tissue were also used for mechanistic investigation.

2. Materials and methods

2.1. Ethics statement

The protocols of this study were approved by the Ethics and Scientific Committees of Harbin Medical University (Harbin, China). Written informed consents were obtained from all the enrolled patients (HMUIRB20170017). The experimental procedures were performed in accordance with the Guide for the Care and Use of Laboratory Animals, published by the US National Institutes of Health (NIH Publication No. 85−23, revised 1996).

2.2. Measurement of circulating levels of TIMP-1, MMP-3 and MMP-8 in patients

Twenty-six cholecystolithiasis patients who received laparoscopic cholecystectomy in the First Affiliated Hospital of Harbin Medical University between February 2017 and March 2018 were enrolled. The study participants were randomly divided into experimental (Berberine; $n = 11-14$) and control (Placebo; $n = 9-12$) groups. The subjects of the experimental group were given 6 mL of polyethylene glycol (PEG) containing 1.5‰ berberine (polyethylene glycol berberine; brand name: Zhan Lian Ping, Heilongjiang

Liaoyuan Science and Technology Co., Ltd., China) in the surface of gallbladder forssa and adjacent intestine, omentum majus and stomach before suturing the incision. The patients of the Placebo group received an equal volume of PEG (medical PEG, brand name: Xian Taihua Medical Co., Ltd., China) without berberine. Plasma from enrolled patients were collected prior to the surgery, as well as 12 and 24 h after administration of berberine. ELISA assays were used to measure plasma concentrations of TIMP-1 (BOSTER, Pleasanton, CA, USA), active MMP-3 (BOSTER) and MMP-8 (BOSTER).

2.3. Primary adhesion rat model

Berberine hydrochloride was obtained from Sigma−Aldrich (St. Louis, MO, USA). The Interceed Absorbable Adhesion Barrier was purchased from Ethicon, Inc. (Somerville, NJ, USA).

Forty-eight healthy Wistar male rats (200−220 g body weight) were used and kept under standard animal room conditions at room temperature (23 ± 1 °C) with constant humidity of 55 ± 5%. For adhesion study, the rats were allocated randomly into five groups (n = 8): control, surgery, pre-BBR, inter-BBR and Interceed groups. The animals were anesthetized intraperitoneally with sodium pentobarbital (3%) at a concentration of 0.15 mL/100 g body weight. The abdomen was then shaved and cleaned with 75% alcohol. After drying, a 3-cm anterior midline ventral laparotomy through the abdominal wall and peritoneum was performed to gain access to the abdominal cavity. Hemorrhagic surface was created on the surface of cecum by abrading with a toothbrush, and normal saline (2.0 mL) was dropped on the cecum immediately after the abrasive surgery. For the control group, normal saline (2.0 mL) was dropped onto the cecum without abrasive surgery (Supporting Information Fig. S1). Then the cecum was placed back to its natural position and the midline incision was closed by suturing. For the pre-BBR group, 3 h before abrasive surgery, 2.0 mL berberine sodium chloride solution (1.5 mg/mL) was intraperitoneally injected into rats. For the inter-BBR group, the same volume/dose of berberine sodium chloride solution was dropped onto the cecum immediately after the abrasive surgery. In the Interceed group, a 3.0 cm × 2.0 cm piece of Interceed was attached to the abraded cecum, and 2.0 mL normal saline was then added onto the Interceed. Seven days later, the animals were euthanized using an overdose of pentobarbital sodium and adhesion score was evaluated. A schematic illustration of the protocols is provided in Fig. S1A.

2.4. Enterolysis rat model

For the experiments involving enterolysis, 32 Wistar rats (200−220 g body weight) were used. The animals were subject to abrasive surgery as described above. One week after the 1st surgery, the animals underwent the second operation for enterolysis. Briefly, adhesion bridges between organs and tissues were lysed using microsurgical instruments and the lysed samples were washed using 0.9% NaCl. The rats with an adhesion score below 5 were excluded. Following the completion of enterolysis, the animals were randomly divided into four groups: control, 2nd surgery, BBR (1.5 mg/mL, added on the surface of lysed cecum immediately after the enterolysis), and Interceed groups. Five days later, the animals were euthanized using an overdose of pentobarbital sodium. A schematic illustration of the protocols is provided in Fig. S1B.

2.5. Evaluation of adhesion formation

A laparotomy was undertaken to assess adhesion formation. The incision was performed at a position remote to the original laparotomy scar to prevent interfering with any adhesions between the abdominal wall and viscera. Abdominal wall was then opened fully for examination of the extent of adhesions. The adhesions were graded by the scoring system developed from previously validated comparisons[11]. This method, taking number, strength and distribution into account, provides an objective measurement of adhesion formation. Scoring was performed by an observer blinded to the study design. Photographs of adhesions were taken for each animal to allow grading of the adhesions by another independent observer who was also blinded to the study design.

2.6. Histological assessments of cecum tissue

Cecum samples were fixed with 4% buffered paraformaldehyde embedded in paraffin, and tissue slices were dehydrated in ascending series of ethanol and cleared in xylene. Then the sections were stained with H&E and Masson trichrome staining for assessing the degree of fibrosis, inflammation, and vascular proliferation microscopically. The cecum samples were fixed with 4% paraformaldehyde, followed by embedding in OCT compound, and cut cross-sectionally into 7-mm-thick sections. Immunofluorescent staining was performed on the abrasive cecum for expression and cellular distribution of fibroblasts specific protein 1 (FSP-1, Abcam, Cambridge, MA, USA). Images were captured using a confocal laser scanning microscope (Media Cybernetics, Bethesda, MD, USA).

2.7. Transmission electron microscopy examinations

The cecum was enucleated and fixed in glutaraldehyde at 4 °C for 24−48 h and then placed in 1% osmium. After dehydration in a graded ethanol series, the tissues were embedded in an epoxy resin mixture at 60 °C for 48 h. Thick sections (1 μm) of cecum were cut and stained with methylene blue for appropriate selection of specific regions for further study, and thin sections (100 nm) were obtained from the peripapillary sclera and placed on copper mesh grids for TEM examinations at 75 kV (JEM-1200EX; JEOL, Tokyo, Japan).

2.8. Primary culturing of fibroblasts from adhesion tissue and transfection

The adhesive tissue was rapidly excised and cleaned in Hanks liquid containing 100 U/mL penicillin and 100 μg/mL streptomycin. Then the tissue was cut into tissue blocks of 0.5−1.0 mm^3 and 12−15 tissue blocks were placed evenly and tightly in the culture flask containing 5 mL Dulbecco's modified Eagle's medium (DMEM) supplemented with 10% fetal bovine serum, 100 U/mL penicillin and 100 μg/mL streptomycin. The side of adhered tissue blocks was upturned to avoid touching the culture medium. The tissue blocks were incubated at 37 °C in a humidified atmosphere of 5% CO_2 and 95% air. After 2.5 h, the culture flask was slightly turned over, and the tissue blocks were cultured in the medium for 3−5 days. Fibroblasts were separated from the tissue blocks, which were taken out when fibroblasts grown to 80% confluency. The fibroblasts were subcultured for subsequent experiments. For transfection, the fibroblasts were starved in serum-free medium for 24 h. si-TIMP-1 (Invitrogen, Carlsbad, CA, USA)

was transfected into the cells with X-treme GENE siRNA transfection reagent (Shanghai GenePharma, Co., Ltd., Shanghai, China) according to the manufacturer's instructions. TIMP-1-overexpressing pcDNA3.1-plasmid (100 nmol/L) was transfected into fibroblasts using Lipofectamine 2000 reagent (Invitrogen) according to the manufacturer's instructions. After 6 h of transfection, the medium was replaced by fresh one with or without BBR (Beijing Solarbio Science & Technology Co., Ltd., Beijing, China) for 24 h. The sequence of TIMP-1 siRNA is 5′-ATG-CATCGATCACTAGCTT-3′.

2.9. Western blot analysis

Protein samples were loaded at 100 μg/well into a 10% SDS-PAGE gel for electrophoresis and transferred onto nitrocellulose membranes (PALL, New York, NY, USA). Next, the membranes were blocked in the 5% defatted milk for 2 h and incubated on a shaker at 4 °C overnight with the primary antibody, TIMP-1 (Abcam), MMP-3 (Abcam), MMP-8 (Abcam), or GAPDH (Zhongshanjinqiao, Inc., Beijing, China) as an internal control.

2.10. Quantitative real-time PCR (qRT-PCR)

QRT-PCR was used to determine the levels of *Vegfα*, collagen 1, collagen 3 transcripts. Total RNA was extracted by TRIzol reagent (Invitrogen) according to manufacturer's instructions. The SYBR Green Realtime PCR Master Mix Kit (Toyobo, New York, NY, USA) was used for real-time PCR amplification for relative quantification of RNAs. GAPDH was used as an internal control. The sequences of primer pairs used in our study are as follows:

Collagen 1: forward 5′-AAGGCTCCCCTGGAAGAGAT-3′ and reverse 5′-CAGGATCGGAACCTTCGCTT-3′; Collagen 3: forward 5′-AGTGGCCATAATGGGGAACG-3′ and reverse 5′-CACCTTTGTCACCTCGTGGA-3′

Vegfα: forward 5′-TCGCGAGACGCAGCGACAAG-3′ and reverse 5′-CAGCGCGACTGGTCCGATGA-3′

2.11. Molecular docking

The crystal structures of TIMP-1 (PDB: 1uea) were downloaded from RCSB Protein Data Bank (http://www.rcsb.org/). The structures of TIMP-1 were prepared with the biopolymer tool of Sybyl-X 2.0 (Tripos Inc., St Louis, MO, USA). Hydrogen atoms were added and AMBER FF99 charges in TIMP-1 protein were calculated. The water in protein was deleted. A 1000-iteration minimization of the hydrogen atoms was followed by a 100-ps molecular dynamics simulation to refine the positions of targets. Inputted ligand (berberine) file format was mol2 for all docking programs under investigation. A SFXC file was built using the PDB prepared protein structure. The protocol was generated using the ligand with a threshold of 0.50 and bloat set to 0 (default settings). Cscore calculations were enabled on Surflex docking runs. Additional starting conformations per molecular were set to 10, and Angstroms to expand search grid were 6. Max conformations per fragment were set to 30, Max number of rotatable bonds per molecular to 150, and the maximum number of poses per ligand to 50. The minimum RMSD between final poses was set to 0.05.

2.12. Surface plasmon resonance (SPR)

Ligand/protein binding analysis was performed using an OpenSPR localized surface plasmon resonance (LSPR) biosensor (Nicoya Life Science Inc., Kitchener, Canada). TIMP-1 served as a receptor and was immobilized to gold nanoparticles on a COOH sensor chip using standard 1-ethyl-3-(3-dimethylpropyl)-carbodiimide (EDC) plus *N*-hydroxysuccinimide (NHS) coupling chemistry. TIMP-1 of 100 μL (50 μg/mL) in activation buffer was introduced into the sensor chip at a flow rate of 20 μL/min with 20 mmol/L Tris-HCl, pH 7.4 as the running buffer. Any remaining activated carboxyl groups were deactivated by treatment with OpenSPR deactivation buffer. The analytic running buffer was comprised of 20 mmol/L Tris−HCl, pH 7.4, 210 mmol/L NaCl, 0.05% (*w*/*v*) Tween 20 and 0.1% (*w*/*v*) BSA. During optimization experiments, analyte (100 μL, BBR 12.5−100 μg/mL) was introduced into a receptor-bound sensor chip at flow rates between 20 and 150 μL/min. Sensorgram traces of BBR:TIMP-1 interaction were recorded and analyzed using the built-in TraceDrawer software package (Ridgeview Instruments, Uppsala Sweden). Ligand/sensor chips were regenerated between each injection of analyte using 10 mmol/L HCl at a flow rate of 100 μL/min.

2.13. Data analysis

The data are shown as mean ± SEM. Statistical comparisons among multiple groups were performed by one-way ANOVA followed by Turkey's Multiple Comparison Test (GraphPad Prism 5.0, San Diego, CA, USA). Comparisons between different groups in tables were applied using the Kruskal−Wallis H and the Mann−Whitney U test by SPSS 19.0. $P < 0.05$ indicates a statistically significant difference. Group assignments, data recording and data analysis were blinded to the operator.

3. Results

3.1. BBR reduces postoperative adhesion in rats

To investigate the effects of BBR in a rat mode of intestinal adhesion, a predetermined adhesion measurement score was used to assess the severity and incidence of adhesion[10]: grade 0, no adhesions; grade 1, loose, filmy adhesions that can be separated by blunt dissection; grade 2, adhesions requiring, <50% sharp dissection for separation; grade 3, adhesions requiring >50% sharp dissection for separation; grade 4, serosal injury; and grade 5, full thickness injury. Examples of photographs taken from post-mortem evaluation of adhesions on day 7 after surgery are displayed in Fig. S1A, and the results on adhesion severity are presented in Table 1. Statistically significant differences were found among the groups in terms of the incidence and severity of adhesion formation. Rats of the abrasive surgery group showed the most severe adhesions between the abraded cecum and the abdominal wall lesion, of which four rats had an adhesion score over 4. The adhesion was remarkably alleviated by BBR pre-treatment and internal treatment, compared with that without treatment. The peritoneal adhesion was completely prevented in 5 out of 7 rats by BBR treatment 3 h before abrasive surgery (Pre-BBR), similar the effects on prevention of primary adhesion elicited by Interceed (3.0 cm × 2.0 cm; a bio-membrane used to cover up the injured area of cecum). While 3 out of 7 rats were

Table 1 Distribution of adhesion scores indicating the adhesion severity and adhesion area in the five different groups: Sham, Surgery, Pre-BBR, Inter-BBR, and Interceed groups.

Group	Adhesion score					
	0	1	2	3	4	5
Sham	7	0	0	0	0	0
Surgery***	0	0	1	2	2	2
Pre-BBR$^{\#\#\#}$	5	2	0	0	0	0
Inter-BBR$^{\#\#}$	3	3	1	0	0	0
Interceed$^{\#\#\#}$	5	2	0	0	0	0

The adhesion at 5 days postoperation was remarkably alleviated with berberine treatment before abrasive surgery (Pre-BBR) or berberine treatment immediately after abrasive surgery (Inter-BBR) and in the Interceed group.
$^{***}P < 0.001$ *vs.* Sham group.
$^{\#\#}P < 0.01$, $^{\#\#\#}P < 0.001$ *vs.* Surgery group.
Comparisons between different groups were applied using the Kruskal–Wallis H and the Mann–Whitney U test by SPSS 19.0.

completed healed after administration of BBR by dropping onto the cecum immediately after the abrasive surgery. A schematic illustration of the experimental protocols with the primary adhesion rat model is provided in Supporting Information Fig. S2A to enhance the clarity of descriptions. The concentration of BBR at 1.5 mg/mL was chosen for the present study based on the validated effective dosage for preventing adhesion formation reported in our published study[10].

3.2. *BBR reduces cicatricial adhesion reformation after enterolysis in rats*

Reformation of adhesion after enterolysis is believed to be a more virulent pathological process than primary adhesion formation[12]. Reduction of adhesion reformation is less easily sustained than *de novo* formation[13]. We found that 67% rats with peritoneal adhesion suffered serious adhesion reformation (grade 5) 5 days after enterolysis, and strikingly, this adhesion reformation was significantly prevented by BBR pretreatment: only 50% of the rats with enterolysis had adhesion reformation (Fig. S1B). By comparison, Interceed had only a weak effect on adhesion reformation, as most of rats had adhesion reformation with score of 2–3. A schematic illustration of the experimental protocols with the enterolysis rat model is presented in Fig. S2B. The results on adhesion severity are summarized in Table 2.

Table 2 Distribution of adhesion scores indicating the adhesion severity and adhesion area in the four different groups: Sham, Surgery, BBR, and Interceed groups.

Group		Adhesion score					
		0	1	2	3	4	5
Sham	Enterolysis	6					
	Treatment	6					
Surgery	Enterolysis						6
	Treatment		1			1	4
BBR*	Enterolysis						6
	Treatment	3	1	1	1		
Interceed	Enterolysis						6
	Treatment		1	2	2	1	

The adhesion reformation at 7 days after enterolysis was remarkably alleviated with BBR treatment.
$^{*}P < 0.05$ *vs.* Surgery group. Comparisons between different groups were applied using the Kruskal–Wallis H and the Mann–Whitney U test by SPSS 19.0.

3.3. *BBR suppresses fibrosis, inflammation and vascular proliferation during intestinal adhesion formation*

To explore the cellular and subcellular mechanisms underlying the anti-adhesion efficacy of BBR, we first examined the histological changes of cecum by H&E and Masson trichrome staining. As revealed by H&E staining, the surgery procedures caused apparent thickening of serosa layer, florid and dense connective tissue, increased the number of admixed lymphocytes, plasma cells, eosinophils, and neutrophils, as well as numerous admixed inflammatory cells with microabscesses. Intense vascular proliferation and congestion were also present, indicating the occurrence of severe inflammatory process in the surgery group compared with the control group. Pre-BBR, inter-BBR and Interceed reduced the inflammatory response and the mild proliferation of the blood vessels (Fig. 1A). Masson trichrome staining of the cecum in the surgery group showed massive collagen production and deposition (blue) in serosa. Pre-BBR, inter-BBR and Interceed remarkably attenuated fibrin and collagen deposition of the cecum samples (Fig. 1B and C). Consistently, these treatments all significantly mitigated the surgery-induced increases in the mRNA levels of collagens 1 and 3 (Fig. 1D and E). In addition, they also prevented the abnormal upregulation of transcript level of *Vegfα* stimulated by surgery (Fig. 1F).

3.4. *BBR suppresses fibrosis, inflammation and vascular proliferation during post-enterolysis adhesion reformation*

Following enterolysis, the second surgery caused prominent regeneration of vessels, accumulation of inflammatory cells and damages of muscle layers (both longitudinal and circular muscle layers) in cecum (Fig. 2A). BBR and Interceed remarkably reduced these adverse alterations in serosa and adhesion tissues. On the other hand, a large amount of collagen accumulated in cecum after post-enterolysis surgery, which invaded from submucosal layer into sarosal layer. Compared to Interceed, BBR produced a greater effect on reducing collagen accumulation in adhesion sites (Fig. 2B and C). Strikingly, the cecum muscle layer with BBR treatment remained well organized and had fewer damages compared to the non-treated enterolysis group, whereas Interceed did not ameliorate the damages caused by post-enterolysis surgery. In agreement with the above observations, BBR produced greater magnitudes of repressing effects on the abnormal expression upregulation of collagen 1 and collagen 3 transcripts induced by post-enterolysis surgery (Fig. 2D and E). Moreover, both BBR and Interceed effectively prevented post-enterolysis upregulation of VEGFα (Fig. 2F).

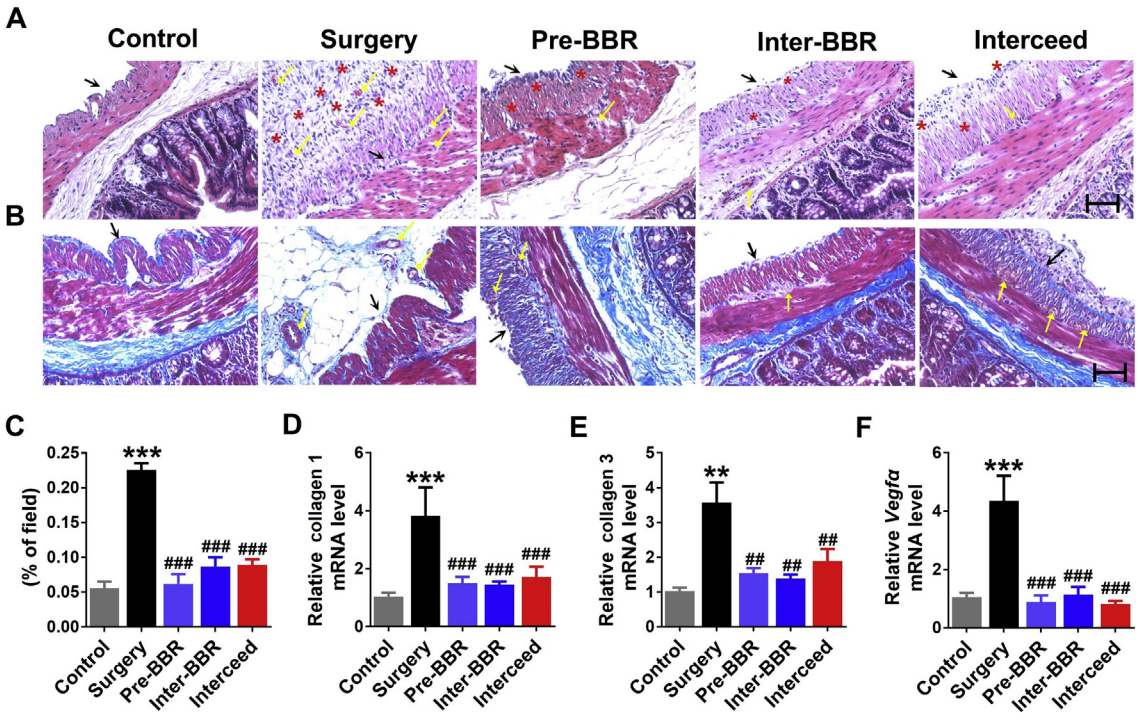

Figure 1 Preventive effect of Pre-BBR and Inter-BBR on primary adhesion. (A) Hemotoxylin and eosin (H&E) staining (magnification 400 ×) showing the inhibitory effects of BBR (100 μmol/L) and Interceed on vascular proliferation and congestion (yellow arrows), and on giant cells with increased numbers of admixed lymphocytes, plasma cells, eosinophils, and neutrophils and numerous admixed inflammatory cells with microabscesses (red asterisks). Black arrows point to the serosa layer. Scale bar: 10 mm. (B) Masson trichrome staining (magnification 400 ×) showing the effects of BBR and Interceed on reducing fibrosis and collagen deposition (blue) in the mesenchymal layer, mucosa layer, submucosal areas, and muscularis propria. Yellow arrows point to vascular proliferation and congestion, and black arrows to the serosa layer. Scale bar: 10 mm. (C) Preventive and inhibitory effects of Pre-BBR (100 μmol/L) and Inter-BBR (100 μmol/L) on collagen contents in rat cecum. (D) Repressive effects of BBR on the mRNA level of collagen 1 in cecum. (E) Repressive effects of BBR on the mRNA level of collagen 3 in cecum. (F) Repressive effects of BBR on the mRNA level of *Vegfα* (vascular endothelial growth factor α) in cecum. Note that BBR and Interceed produced nearly the same magnitudes of effects. The data are presented as mean ± SEM, $n = 3-6$; $^{**}P < 0.01$, $^{***}P < 0.001$ *vs*. control group; $^{\#\#}P < 0.01$, $^{\#\#\#}P < 0.001$ *vs*. surgery group.

3.5. *BBR upregulates MMP-3/8 by inhibiting TIMP-1*

We then continued our study to elucidate the signaling mechanisms for the preventive and anti-adhesion reformation effects of BBR. Considering the prominent effects of BBR on reducing collagen accumulation in adhesion samples, we speculated that MMP might be involved in this process. It is known that TIMP-1 acts as a potent inhibitor of several MMPs[14], of which MMP-3 and MMP-8 share the same domain structure of active core and are the primary proteinases for collagen 1 and collagen 3[15,16]. As illustrated in Fig. 3, in the surgery group, TIMP-1 protein level was largely increased in adhesion tissue and rat plasma (Fig. 3A and B). Active MMP-3 was detectable both intracellularly and extracellularly (due to secretion from the cells), whereas active MMP-8 was found existing only extracellularly. Active MMP-3 levels were considerably decreased in both cells and plasma of the surgery group. Similarly, plasma active MMP-8 was also remarkably decreased. The dysregulation of TIMP-1, MMP-3 and MMP-8 was reversed by pre-BBR and inter-BBR treatments (Fig. 3C and D).

In rats with post-enterolysis adhesion reformation, the protein level of TIMP-1 was upregulated (Fig. 4A and B), whilst those of active MMP-3 and MMP-8 were downregulated, and these changes were all reversed by BBR (Fig. 4C and D). Unexpectedly but not surprisingly, Interceed affected the expression of TIMP-1 and MMP in the settings of neither adhesion formation nor post-enterolysis adhesion reformation models.

Fibroblasts are active during wound healing process resulting in increased collagen secretion and fibrous bridges formation[17]. We found prominent enhancement of immunofluorescent labeling of FSP-1 indicative of fibroblast accumulation in adhesion tissues (Supporting Information Fig. S3A). Meanwhile, the results obtained from transmission electron microscopy also revealed a pronounced enrichment of activated fibroblasts in cecal serosa after surgery compared to the control group (Fig. S3B). The activated fibroblasts were in polygonal morphology and they were enlarged in size with a high proportion of nucleoplasm, thick mitochondria, abundant rough endoplasmic reticulum and Golgi complex. In the primary cultured fibroblasts isolated from adhesion tissues, BBR treatment for 24 h remarkably decreased the protein level of TIMP-1 in a concentration-dependent manner (Fig. 5A), and immunofluorescent staining indicated the downregulation of TIMP-1 in both nucleus and cytoplasm (Fig. 5B). In addition, TIMP-1 concentration in the culture medium of primary cultured fibroblasts was also decreased as assessed by ELISA (Fig. 5C), indicating the reduced secretion of this protein out to extracellular space. In sharp contrast, the protein level of active MMP-3 was elevated by TIMP-1 siRNA (si-TIMP1) to silence

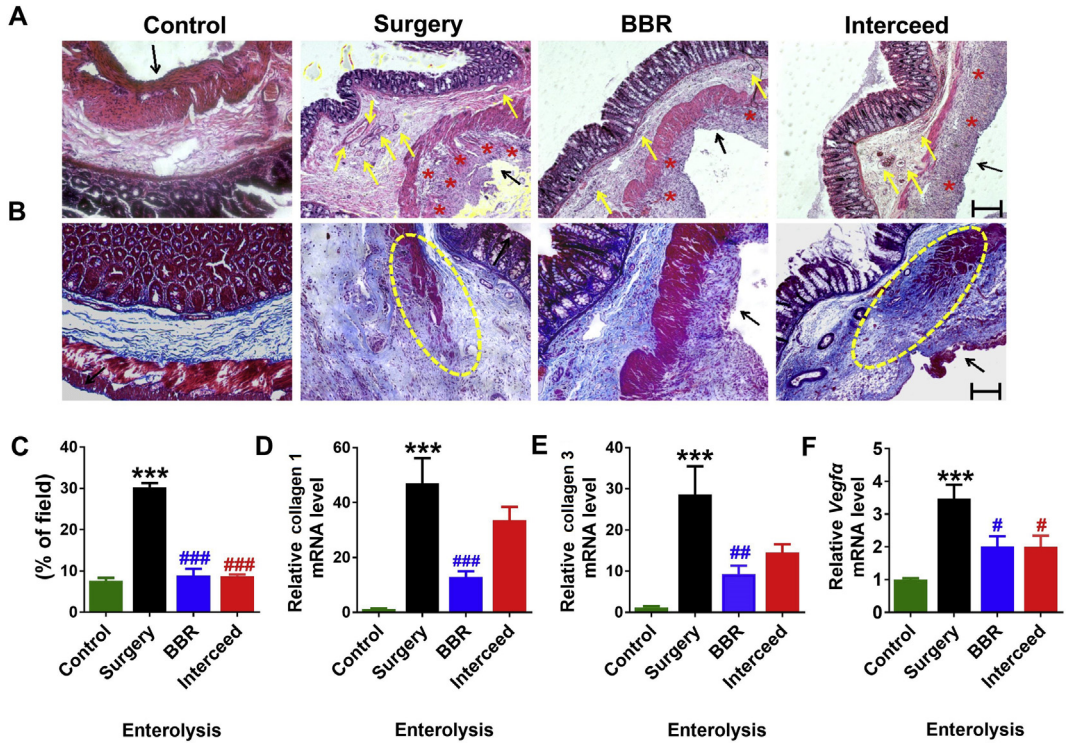

Figure 2 Effects of BBR on the pro-adhesive alterations induced by enterolysis. (A) Hemotoxylin and eosin (H&E) staining (magnification 200 ×) showing the inhibitory effects of BBR (100 μmol/L) on vascular proliferation and congestion (yellow arrows), and on giant cells with increased numbers of admixed lymphocytes, plasma cells, eosinophils, and neutrophils and numerous admixed inflammatory cells with micro-abscesses (red asterisks) following enterolysis. Black arrows point to the serosa layer. Scale bar: 10 mm. (B) Masson trichrome staining (magnification 400 ×) showing the effects of BBR on reducing fibrosis and collagen deposition (blue) in the mesenchymal layer, mucosa layer, submucosal areas, and muscularis propria following enterolysis. Yellow arrows point to vascular proliferation and congestion, and black arrows to the serosa layer. Yellow ellipse represents injured muscle layers (both longitudinal and circular muscle layers). Scale bar: 10 mm. (C) Preventive and inhibitory effects of Pre-BBR (100 μmol/L) and Inter-BBR (100 μmol/L) on collagen contents in rat cecum following enterolysis. (D) Repressive effects of BBR on the mRNA level of collagen 1 in cecum following enterolysis. (E) Repressive effects of BBR on the mRNA level of collagen 3 in cecum following enterolysis. (F) Repressive effects of BBR on the mRNA level of *Vegfα* in cecum. Note that BBR produced greater magnitudes of effects than Interceed. The data are presented as mean ± SEM, $n = 3-6$; $^{***}P < 0.001$ *vs*. control group; $^{\#}P < 0.05$, $^{\#\#}P < 0.01$, $^{\#\#\#}P < 0.001$ *vs*. surgery group.

endogenous TIMP-1 (Fig. 5A), and so was the content of active MMP-3 in the culture medium (Fig. 5D). Active MMP-8 was also elevated in the culture medium (Fig. 5E).

We reasoned that if BBR indeed acted through inhibiting TIMP-1, then forced expression of TIMP-1 should be able to counteract the effects of BBR. To examine this notion, we transfected the TIMP-1-containing plasmid (pcDNA3.1-TIMP-1) for overexpression in fibroblasts. The results in Fig. 6A confirm the overexpression of TIMP-1 by pcDNA3.1-TIMP-1 and demonstrate the effectiveness of BBR to mitigate the overexpression. As expected, overexpression of TIMP-1 caused a significant decrease in the level of active MMP-3. BBR at a higher concentration (100 μmol/L) not only blocked out the overexpression of TIMP-1 but also downregulated the endogenous expression of TIMP-1. Correspondingly, the level of active MMP-3 was significantly increased by BBR (Fig. 6A). The Western blot results on the effects of BBR on TIMP-1 overexpression and intrinsic expression were confirmed by immunocytochemistry in Fig. 6B. Furthermore, TIMP-1 content that increased by TIMP-1 overexpression in culture medium was also significantly reduced by BBR treatment (Fig. 6C). In addition, overexpression of TIMP-1 diminished the extracellular contents of active MMP-3 and MMP-8, and BBR rescued such a change in a concentration-dependent fashion (Fig. 6D and E). Our data indicate that TIMP-1 overexpression suppressed the activating effects of BBR on MMP-3 and MMP-8, or in other words, BBR repressed TIMP-1 expression to activate MMP-3/8.

To further investigate the possible regulatory mechanism of BBR on TIMP-1. We performed molecular docking simulation on BBR and TIMP-1 using SYBYL 2.0 software. The results indicate that BBR fits well into the active region of TIMP-1 (PDB: 1uea) and can form H-bond with residues Tyr136 and Phe132 (Supporting Information Fig. S4A). The calculated CScore of 4 and Polar value of 1.36 indicate optimal polar interaction between BBR and TIMP-1, and Crash value of −0.85 reflects the degree of intermolecular collision. Tyr136 and Phe132 residues are located adjacent to the C-connector loop of TIMP-1, forming part of the active motif that interacts with MMPs. We therefore proposed that BBR can bind directly to the active motif of TIMP-1 and induce conformational changes of the latter, followed by protein degradation. We then examined this hypothesis using SPR analysis to determine the binding potential. The SPR data clearly showed that BBR interacts with TIMP-1 to form a stable complex with an affinity constant (K_D) of 3×10^{-5} mol/L. The association rate

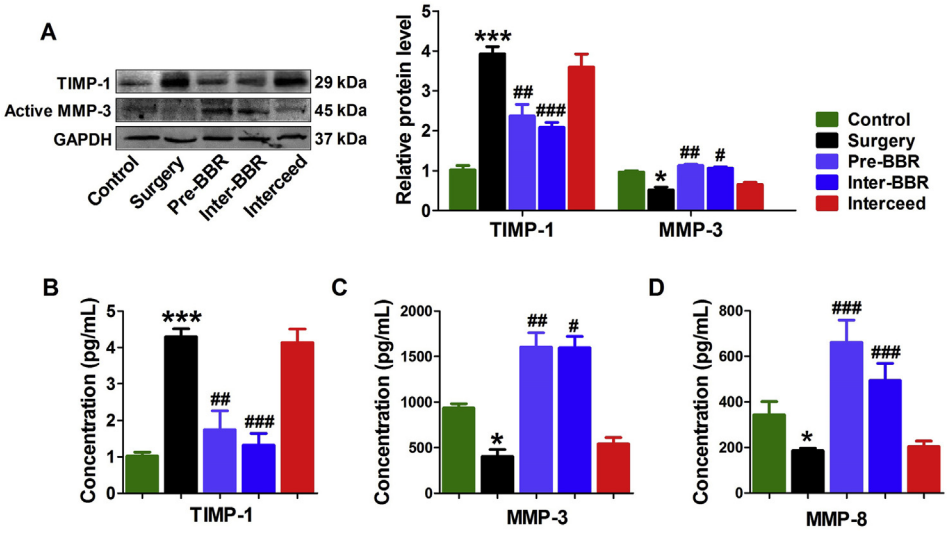

Figure 3 Effects of BBR treatments on the pro-adhesive alterations of plasma tissue inhibitor of metalloproteinases 1 (TIMP-1) and matrix metallopeptidase 3/8 (MMP-3/MMP-8) levels induced by abrasive abdominal surgery in rats. Rats intraperitoneally injected with 2.0 mL BBR (1.5 mg/mL) 3 h prior to abrasive surgery were designated as BBR pretreatment (Pre-BBR) and rats administered with BBR directly onto the cecum immediately after the abrasive surgery were assigned as Inter-BBR. (A) Western blot results showing the prevention by Pre-BBR and reversal by Inter-BBR of surgery-induced upregulation of TIMP-1 and the lack of effect of Interceed. (B) Pre-BBR prevented and Inter-BBR decreased the surgery-induced elevation of plasma TIMP-1 concentration in rats, as measured by ELISA. (C) Pre-BBR and Inter-BBR increased the plasma level of active MMP-3, preventing and abrogating the surgery-induced decreases of MMP-3. (D) Pre-BBR and Inter-BBR increased the plasma level of active MMP-8, preventing and abrogating the surgery-induced decreases of MMP-8. Note the lack of effects of Interceed on plasma levels of TIMP-1 and MMP-3/MMP-8. The data are presented as mean ± SEM, $n = 3$–5; $^{*}P < 0.05$, $^{***}P < 0.001$ *vs.* control group; $^{\#}P < 0.05$, $^{\#\#}P < 0.01$, $^{\#\#\#}P < 0.001$ *vs.* surgery group.

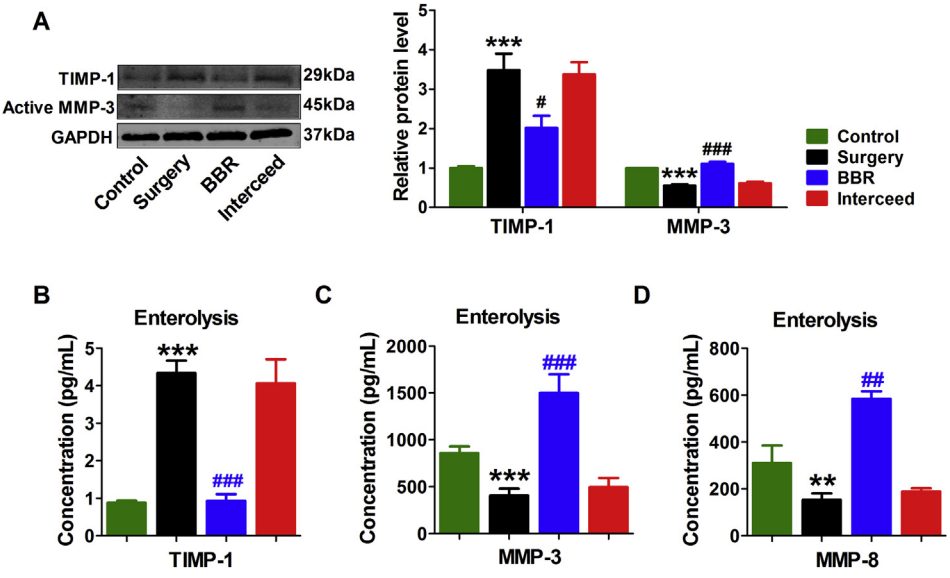

Figure 4 Effects of BBR on the pro-adhesive alterations of plasma TIMP-1 and MMP-3/MMP-8 levels induced by the second abdominal surgery following enterolysis in rats. (A) Western blot results showing the reversal of surgery-induced upregulation of TIMP-1 by BBR (50 μmol/L) and the lack of effect of Interceed. (B) BBR decreased the 2nd surgery-induced elevation of plasma TIMP-1 concentration after enterolysis process in rats, measured by ELISA. (C) BBR increased the plasma level of active MMP-3, abrogating the decrease induced by the 2nd surgery after enterolysis process in rats. (D) BBR increased the plasma level of active MMP-8, abrogating the decrease induced by the 2nd surgery after enterolysis process in rats. Note the lack of effects of Interceed on plasma levels of TIMP-1 and MMP-3/MMP-8. The data are presented as mean ± SEM, $n = 3$; $^{**}P < 0.01$, $^{***}P < 0.001$ *vs.* control group; $^{\#}P < 0.05$, $^{\#\#}P < 0.01$, $^{\#\#\#}P < 0.001$ *vs.* surgery group.

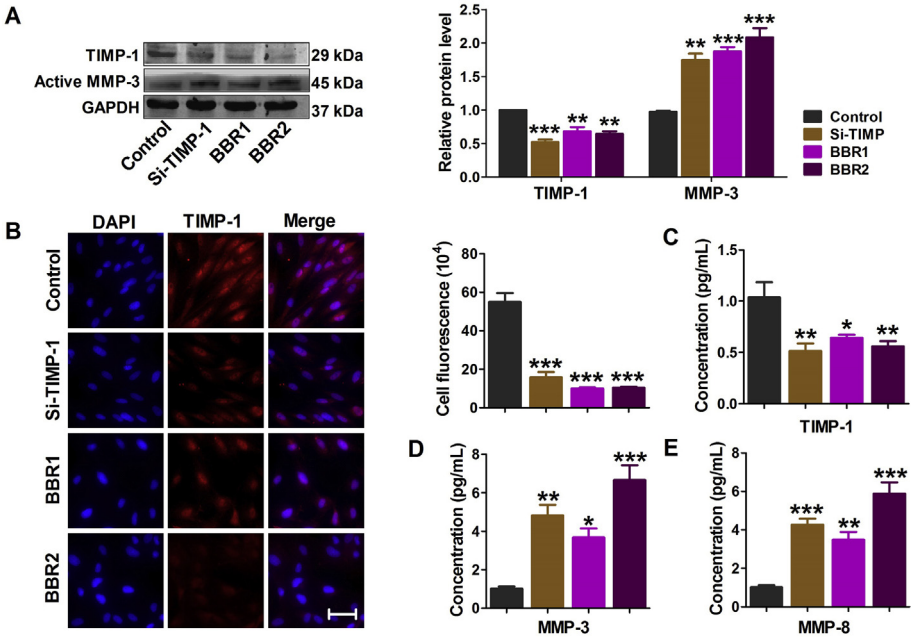

Figure 5 BBR upregulates MMP-3/MMP-8 and downregulates TIMP-1 expression in fibroblasts. (A) Western blot results showing the downregulating effect of BBR (BBR1: 50 μmol/L and BBR2: 100 μmol/L) on TIMP-1 and upregulating effects on active MMP3. Si-TIMP-1:TIMP-1 siRNA. (B) Representative images of immunostaining of TIMP-1 (red; left panel) in fibroblasts and statistical data (right panel) displaying the decreases of TIMP-1 protein by BBR. The nuclei were stained blue with DAPI. Scale bars: 10 μm. (C) BBR decreases the concentration of TIMP-1 in the culture medium of fibroblasts, measured by ELISA. (D) BBR increases the concentration of active MMP-3 in the culture medium of fibroblasts. (E) BBR decreases the concentration of active MMP-8 in the culture medium of fibroblasts. The data are presented as mean ± SEM, $n = 3-5$; $^{*}P < 0.05$, $^{**}P < 0.01$, $^{***}P < 0.001$ *vs*. control group.

constant (K_a) is 1.53×10^2 L/mol·s, dissociation rate constant (K_d) is 4.58×10^{-3}/s (Fig. S4B).

3.6. *BBR decreases plasma TIMP-1 level, increases plasma MMP-8 and MMP-3 levels in patients*

While the results presented above strongly suggest that BBR possesses anti-adhesion formation and post-enterolysis adhesion reformation properties due to its ability to activate MMP-3/MMP-8 through downregulating TIMP-1, we wanted to implicate these findings to clinical practice. Secreted forms of TIMP-1, MMP-3 and MMP-8 exist extensively in human plasma and have been proposed to be biomarkers for several diseases. To this end, we investigated the effects of BBR on circulating levels of TIMP-1 and its downstream factors MMP-3 and MMP-8 in human subjects.

We enrolled 26 cholecystolithiasis patients who received laparoscopic cholecystectomy with or without BBR (polyethylene glycol berberine, brand name: Zhan Lian Ping) treatment in the First Affiliated Hospital of Harbin Medical University between June 2017 and March 2018. The study participants were randomly divided into experimental (BBR) and control (placebo) ($n = 9-12$) groups. The subjects of the experimental group were treated with 6 mL of Zhan Lian Ping (6 mL PEG containing 1.5‰ berberine). The patients of the placebo group received an equal volume of medical PEG. Plasma concentrations of active TIMP-1, MMP-8 and MMP-3 were measured prior to the surgery, as well as 12 and 24 h after administration of BBR (Fig. 7). In patients treated with placebo, the plasma TIMP-1 levels were increased by 5.4-fold 12 h after surgery and 6.1-fold 24 h after surgery (Fig. 7A). In contrast, in patients of the BBR group after surgery, plasma levels of TIMP-1 were reduced to 67% at 12 h and 15% at 24 h (Fig. 7A). The patients had significantly decreased plasma levels of MMP-3 to 39% of the placebo value at 12 h and 31% at 24 h after surgery, and BBR rescued the surgery-induced decreases, elevating MMP-3 levels by 1.3-fold at 12 h and by 2.1-fold at 24 h (Fig. 7B). Similarly, MMP-8 was reduced to 17% at 12 h and 14% at 24 h after surgery, and these detrimental alterations were corrected by BBR relative to the placebo group: 1.2-fold elevation at 12 h and 2.1-fold elevation at 24 h after surgery in patients treated with BBR (Fig. 7C).

3.7. *BBR prevents primary adhesion formation and adhesion reformation in a dose-dependent manner*

We then evaluated the dose−response of BBR in treating primary adhesion and adhesion reformation. The dosage of BBR was set as follows: 0.75, 1.5, 3, and 6 mg/mL. For adhesion reformation, 1.5 and 3 mg/mL BBR were used. Berberine sodium chloride solution (2 mL) was dropped onto the cecum immediately after the abrasive surgery or enterolysis. The results demonstrated that BBR effectively prevented adhesion formation and adhesion reformation in a dose-dependent manner (Supporting Information Tables S1 and S2). BBR inhibited inflammation and collagen accumulation at different doses in both adhesion models (Supporting Information Figs. S5 and S6). Moreover, BBR reduced the CD31-positive staining, suggesting an inhibition of blood vessels formation in adhesion tissue (Supporting Information Figs. S7 and S8). As expected, the active TIMP-1 was remarkably decreased in

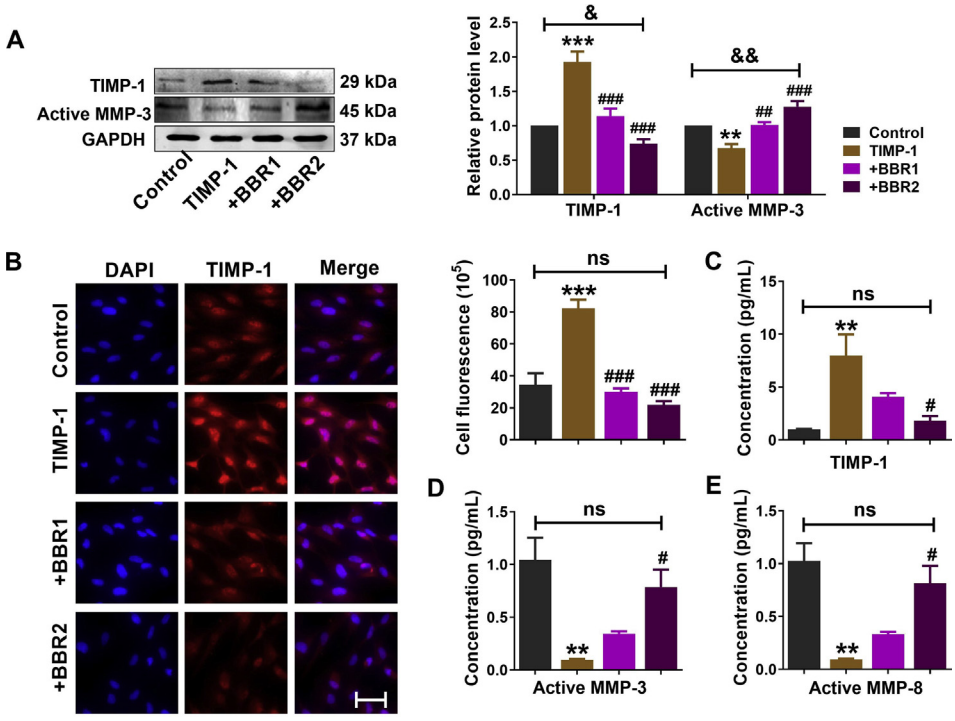

Figure 6 Overexpression of TIMP-1 abolishes the promoting effects of BBR on MMP-3 and MMP-8 activation in cultured fibroblasts. (A) Western blot results depicting the effects of BBR on the level of active MMP-3 in the presence of TIMP-1 overexpression. Cells were transfected with pcDNA3.1 plasmid carrying the TIMP-1 gene for overexpression. +BBR1: 50 μmol/L BBR in cells with TIMP-1 overexpression; +BBR2: 100 μmol/L BBR in cells with TIMP-1 overexpression. (B) Immunostaining of TIMP-1 in fibroblasts (red) showing the effectiveness of BBR to abolish the overexpression of TIMP-1. The nuclei were stained blue with DAPI. Scale bar: 10 μm. Concentration of TIMP-1 (C), MMP-3 (D) and MMP-8 (E) in the supernatant of fibroblast culture medium, determined by ELISA. The data are presented as mean ± SEM, $n = 3-6$; $^{**}P < 0.01$, $^{***}P < 0.001$, $^{\&}P < 0.05$, $^{\&\&}P < 0.01$ *vs*. control group; $^{\#}P < 0.05$, $^{\#\#}P < 0.01$, $^{\#\#\#}P < 0.001$ *vs*. TIMP-1 group. "ns" represents non-significant difference between the control and BBR2 groups.

rat plasma with graded increases in BBR dosages, whereas MMP-3 and MMP-8 were activated by BBR in a dose-dependent manner (Supporting Information Figs. S9 and S10).

4. Discussion

In the present study, we investigated the roles of the TIMP-1/MMP3/8 axis in mediating the effects of BBR on primary adhesion formation and adhesion reformation after enterolysis. First, our results showed that BBR treatment before or immediately after abrasive injury prevented primary adhesion formation. More ECM deposition and greater tissue damage were observed with adhesion reformation than with primary adhesion. BBR produced greater inhibitory effect on adhesion reformation than Interceed did. Increase in TIMP-1 results in decreases in MMP-3/MMP-8, contributing to primary adhesion formation and reformation after enterolysis. Upregulating MMP-3/MMP-8 through inhibiting TIMP-1 by BBR might partially account for the preventive effects of this compound on adhesion formation.

Peritoneal adhesion and cicatricial adhesion reformation after abdominal surgery are the consequence of excessive ECM deposition of and of inflammation as well, that facilitates the progression of a variety of complications, such as chronic abdominopelvic discomfort, pain, and infertility[18]. Meanwhile, reformation of adhesions after enterolysis is a more virulent pathological process than primary adhesion formation. Some studies reported that adhesive tissue collected in adhesion reformation sites revealed more excessive fibrin and collagen accumulation, possibly reflecting higher adhesive propensity. Such a high adhesive potential might be a reason that reduction of adhesion reformation is less easily sustained than primary adhesion formation in animal models[19]. Similarly, in our study, we also observed significant difference between adhesion reformation and primary adhesion formation in histological features. As presented by H&E and Masson staining, adhesion reformation rats had more productive collagens and crushed tissue integrity in the adhesive cecum. These phenomena suggest that with more extensive tissue damage, Interceed is less effective to reduce adhesion reformation.

We have previously reported that BBR had a compatible anti-adhesion effects with Interceed in primary adhesion rats by inhibiting inflammation process[10]. Here, our results showed that intra-abdominal injection of BBR before abrasive adhesion surgery had a similar effect with BBR treatment immediately after the surgery. In addition, adhesion reformation after enterolysis was remarkably prevented by BBR. Meanwhile, BBR significantly decreased collagen accumulation and reserved muscle layers damage as well. By comparison, Interceed failed to reduce adhesion scores in the reformation model; neither did it affect collagen production nor tissue integrity in adhesive cecum. These results were consistent with the hypothesis that adhesion formation and reformation represent different processes with the latter being more difficult to prevent[19,20]. Moreover, our findings also suggest that the anti-adhesion mechanism for BBR might differ

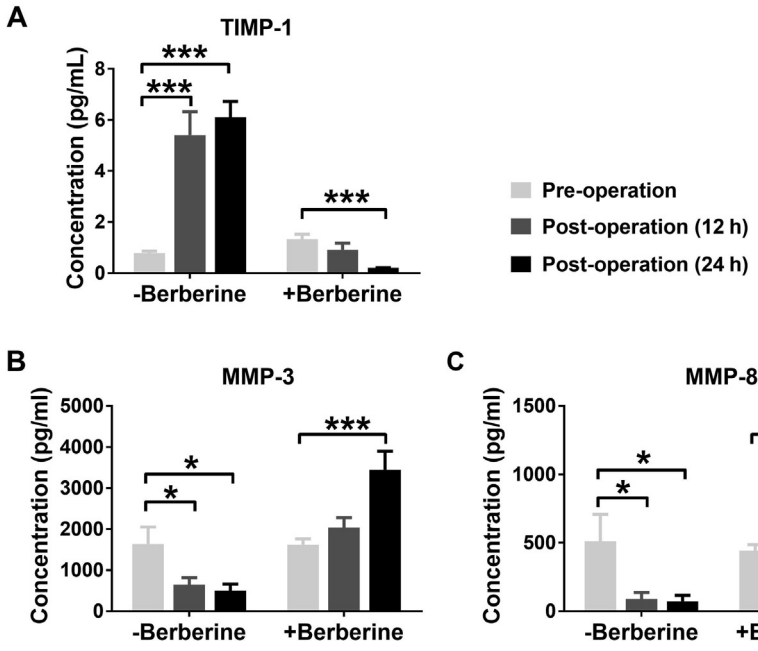

Figure 7 Effects of BBR on plasma contents of TIMP-1 and MMP-3/MMP-8 in cholecystolithiasis patients after laparoscopic cholecystectomy. (A) BBR suppressed the elevation of plasma TIMP-1 level induced by abdominal surgery. (B) BBR rescued the surgery-induced decrease in plasma level of active MMP-3. (C) BBR rescued the surgery-induced decrease in plasma level of active MMP-8. The data are presented as mean ± SEM, $n = 9-14$; $^{*}P < 0.05$, $^{***}P < 0.001$ *vs*. pre-operation group.

from that for Interceed. Indeed, studies have reported that the reduction of adhesion reformation is less effective than the reduction of primary adhesion formation using anti-adhesive barriers in both clinical and animal studies. Interceed is a pro-coagulant and it can cause fibrin deposition at sites of incomplete haemostasis[21]. Another difference between the two therapeutic approaches is the accumulation of fibroblasts in adhesion sites. After trauma to the peritoneum and intestine, the cell population changes with the maturity of the adhesion tissue, with the initial cell type at days 1−3 being mainly polymorphonuclear leukocytes and on days 5−7 mainly fibroblasts[22,23]. The immunofluorescent staining results in Fig. S3 show that fibroblasts migrated to fibrous bridge in both the surgery and BBR treatment groups. In the Interceed treatment group, a large number of activated fibroblasts, which were physically blocked by the Interceed barrier, aggregated in the serosal layer of cecum. These results partially account for the observation that more abundant collagen accumulated in the cecal serosal layer of Interceed treated rats.

TIMPs are expressed by a variety of cell types and present in most human tissues and body fluids. All four subtypes of TIMPs can act as potent regulators of the proteolytic activity of MMPs by forming non-covalent 1:1 stoichiometric complexes with their target proteases[24,25]. The balance between levels of MMPs and TIMPs controls the extent of local ECM degradation in the periphery of cells and thereby influences cellular processes such as migration, proliferation and survival[26]. MMP-3 is known for its role in controlling the ECM integrity by catalytically degrading structural proteins including laminin, fibronectin, and various types of collagen. In addition, MMP-3 is able to activate pro-MMP1, 3, 7, 8, 9 and 13 for their substantial biological functions[27]. Importantly, secreted MMP-3 can be extracellularly activated and subsequently transported back into the cell. Both intra- and extracellular activities of MMP-3 can be regulated by TIMPs[28,29]. An altered balance between TIMPs and MMP-3 is known to impair wound healing[30]. Collagenase MMP-8 is promptly secreted and activated in the extracellular compartment after synthesis. The major substrate of MMP-8 is collagen types 1, 2 and 3, and this allows MMP-8 to influence the biological activities of many of these substrates, especially in ECM accumulation[31]. In our study, we observed an increase in TIMP-1 activation, and decrease in MMP-3 and MMP-8 activation in patients after surgery, as well as rats with primary adhesion formation and adhesion reformation. BBR treatment reversed the TIMP-1/MMP imbalance by inhibiting TIMP-1 protein expression. Moreover, Evidence has been out there indicating that TIMP-1 is closely related to inflammatory diseases. TIMP-1 participates in the inflammatory response through regulation of inflammatory mediators, thereby affecting the progression of the disease. TIMP-1 induces an increase of neutrophils in the liver *via* promoting CD63 signaling, which in turn strongly promotes liver inflammation and tumor metastasis[32]. Serum TIMP-1 levels are significantly higher in patients with severe sepsis than in healthy controls[33]. TIMP-1 deficiency results in an asthma phenotype with significant increases in the expression of Gal-3, IL-17 and transforming growth factor-β[34]. The interplay between the anti-inflammatory action and the anti-TIMP-1 action during BBR treatment in peritoneal adhesion was also worthy of investigation in further studies.

TIMPs comprise two distinct domains that are each stabilized by three disulfide bonds: N-terminal domain of about 125 amino acids and C-terminal domain of about 65 residues. Mechanistically, the N-terminal domain of TIMP-1 inhibits metalloproteinases by inserting a conserved anchor, comprising its disulfide bond forming[35]. Hence, the results of molecular docking simulated by SYBYL software, indicate that BBR could insert tightly into the active core of TIMP-1 by forming hydrogen bonds

with phenylalanine132 and tyrosine136 residues. SPR detection revealed a strong interaction potent between BBR and TIMP-1 protein. In addition, in rats and cultured fibroblasts, BBR treatment significantly reduced the protein level of TIMP-1. The nuclear magnetic resonance (NMR) structure of free human N-TIMP-1 bound to the catalytic domain of human MMP-3 and MMP-8 had been clearly described[36,37]. Additionally, fibrin, collagen 1 and collagen 3 are common substrates of MMP-3 and MMP-8. MMP-3 and MMP-8 have homologous catalytic hemopexin-like (HPX) domain[38]. As a consequence, the activated MMP-3 and MMP-8 were remarkably increased. TIMP-1 overexpression abolished the activation effects of BBR for MMP-3 and MMP-8. In our models, Interceed did not affect TIMP-1/MMP balance, which might be the reason why Interceed produced smaller effects than BBR on reducing collagen accumulation in adhesion reformation. Moreover, we estimated that the preventive effects of BBR on adhesion reformation were partially dependent on its inhibitory role for ICAM-1, in consideration of our previously published study. However, the effects of BBR on ICAM-1 only contribute to reduce cell-to-cell adhesion and inflammation. Excessive collagen accumulation cannot be reduced by ICAM-1 inhibition. Therefore, we attribute the effects of BBR on TIMP-1 and MMP-3/MMP-8 as the main mechanism for its suppressive action on excessive collagen accumulation in adhesion reformation.

5. Conclusions

The salient findings in the present study supported a novel pharmacological effect of BBR: effectively preventing adhesion formation and cicatricial adhesion reformation after enterolysis in rats. Moreover, our findings revealed the inhibitory effect of BBR on TIMP-1. Suppression of TIMP-1 expression, activation of MMP-8 and MMP-3 could be as a biochemical mechanism for the anti-fibrosis property of peritoneal adhesion. Furthermore, BBR possessed better preventative effects than Interceed for adhesion reformation. These results provided new therapeutic approaches for clinical treatment of primary adhesion or adhesion reformation.

Acknowledgments

This work was supported by the National Nature Science Foundation of China (81570399 and 81773735), the National Key Research and Development Program of China-Traditional Chinese Medicine Modernization Research project (2017YFC1702003, China) and Heilongjiang Outstanding Youth Science Fund (JC2017020, China).

Author contributions

Baofeng Yang and Yong Zhang conceived and designed the study and wrote the manuscript. Xin Liu, Yunwei Wei and Xue Bai performed major experiments and analyzed data. Mingqi Li, Huimin Li, Lei Wang, Shuqian Zhang, Hao Cui and Xia Li performed Western bloting, immunochemistry and qRT-PCR experiments. Tong Zhao and Heng Liu performed primary cell culture and transfection experiments. Yang Liu and Rui Geng collected clinical samples. Hao Cui, Huimin Li, Ranchen Xu performed ELISA experiment. All authors contributed and approved the manuscript.

Conflicts of interest

The authors declare that no competing interest exists.

Appendix A. Supporting information

Supporting data to this article can be found online at https://doi.org/10.1016/j.apsb.2020.02.003.

References

1. Moris D, Chakedis J, Rahnemai-Azar AA, Wilson A, Hennessy MM, Athanasiou A, et al. Postoperative abdominal adhesions: clinical significance and advances in prevention and management. *J Gastrointest Surg* 2017;**21**:1713–22.
2. Diamond MP, Freeman ML. Clinical implications of postsurgical adhesions. *Hum Reprod Update* 2001;**7**:567–76.
3. Sajid MS, Khawaja AH, Sains P, Singh KK, Baig MK. A systematic review comparing laparoscopic *vs* open adhesiolysis in patients with adhesional small bowel obstruction. *Am J Surg* 2016;**212**:138–50.
4. Richards MK, McAteer JP, Drake FT, Goldin AB, Khandelwal S, Gow KW. A national review of the frequency of minimally invasive surgery among general surgery residents: assessment of ACGME case logs during 2 decades of general surgery resident training. *JAMA Surg* 2015;**150**:169–72.
5. Wang R, Shen Q, Li X, Xie C, Lu W, Wang S, et al. Efficacy of Inverso isomer of CendR peptide on tumor tissue penetration. *Acta Pharm Sin B* 2018;**8**:825–32.
6. Cheong YC, Laird SM, Li TC, Shelton JB, Ledger WL, Cooke ID. Peritoneal healing and adhesion formation/reformation. *Hum Reprod Update* 2001;**7**:556–66.
7. Chaturvedi AA, Lomme RM, Hendriks T, van Goor H. Ultrapure alginate gel reduces adhesion reformation after adhesiolysis. *Int J Colorectal Dis* 2014;**29**:1411–26.
8. van den Beukel BA, de Ree R, van Leuven S, Bakkum EA, Strik C, van Goor H, et al. Surgical treatment of adhesion-related chronic abdominal and pelvic pain after gynaecological and general surgery: a systematic review and meta-analysis. *Hum Reprod Update* 2017;**23**:276–88.
9. Kumar A, Ekavali Chopra K, Mukherjee M, Pottabathini R, Dhull DK. Current knowledge and pharmacological profile of berberine: an update. *Eur J Pharmacol* 2015;**761**:288–97.
10. Tsai JM, Sinha R, Seita J, Fernhoff N, Christ S, Koopmans T, et al. Surgical adhesions in mice are derived from mesothelial cells and can be targeted by antibodies against mesothelial markers. *Sci Transl Med* 2018;**10**:eaan6735.
11. Zhang Y, Li X, Zhang Q, Li J, Ju J, Du N, et al. Berberine hydrochloride prevents postsurgery intestinal adhesion and inflammation in rats. *J Pharmacol Exp Therapeut* 2014;**349**:417–26.
12. Koninckx PR, Gomel V, Ussia A, Adamyan L. Role of the peritoneal cavity in the prevention of postoperative adhesions, pain, and fatigue. *Fertil Steril* 2016;**106**:998–1010.
13. Bayhan Z, Zeren S, Kocak FE, Kocak C, Akcılar R, Kargı E, et al. Antiadhesive and anti-inflammatory effects of pirfenidone in postoperative intra-abdominal adhesion in an experimental rat model. *J Surg Res* 2016;**201**:348–55.
14. Townsend KL, Race A, Keane M, Miller W, Dishaw L, Fisher ER, et al. A novel hydrogel-coated polyester mesh prevents postsurgical adhesions in a rat model. *J Surg Res* 2011;**167**:e117–24.
15. Lin XN, Zhou F, Wei ML, Yang Y, Li Y, Li TC, et al. Randomized, controlled trial comparing the efficacy of intrauterine balloon and intrauterine contraceptive device in the prevention of adhesion reformation after hysteroscopic adhesiolysis. *Fertil Steril* 2015;**104**:235–40.

16. Strik C, Stommel MW, Schipper LJ, van Goor H, Ten Broek RP. Long-term impact of adhesions on bowel obstruction. *Surgery* 2016;**159**:1351−9.
17. Behman R, Nathens AB, Byrne JP, Mason S, Look Hong N, Karanicolas PJ. Laparoscopic surgery for adhesive small bowel obstruction is associated with a higher risk of bowel injury: a population-based analysis of 8584 patients. *Ann Surg* 2017;**266**:489−98.
18. Diamond MP. Reduction of postoperative adhesion development. *Fertil Steril* 2016;**106**:994−7.
19. Yang JH, Chen CD, Chen SU, Yang YS, Chen MJ. The influence of the location and extent of intrauterine adhesions on recurrence after hysteroscopic adhesiolysis. *BJOG* 2016;**123**:618−23.
20. Luciano DE, Roy G, Luciano AA. Adhesion reformation after laparoscopic adhesiolysis: where, what type, and in whom they are most likely to recur. *J Minim Invasive Gynecol* 2008;**15**:44−8.
21. Haney AF, Hesla J, Hurst BS, Kettel LM, Murphy AA, Rock JA, et al. Expanded polytetrafluoroethylene (Gore-Tex surgical membrane) is superior to oxidized regenerated cellulose (Interceed TC7+) in preventing adhesions. *Fertil Steril* 1995;**63**:1021−6.
22. Xiao D, Zhang Y, Wang R, Fu Y, Tong Z, Diao H, et al. Emodin alleviates cardiac fibrosis by suppressing activation of cardiac fibroblasts *via* upregulating metastasis associated protein 3. *Acta Pharm Sin B* 2019;**9**:724−33.
23. Ahmad G, Mackie FL, Iles DA, O'Flynn H, Dias S, Metwally M. Fluid and pharmacological agents for adhesion prevention after gynaecological surgery. *Cochrane Database Syst Rev* 2014;**7**:CD001298.
24. Jackson HW, Defamie V, Waterhouse P, Khokha R. TIMPs: versatile extracellular regulators in cancer. *Nat Rev Canc* 2017;**17**:38−53.
25. Derer S, Waetzig GH, Seegert D, Nikolaus S, Schreiber S, Rosenstiel P. A possible link between TIMP-1 induction and response to infliximab. *Gut* 2009;**58**:888−9.
26. Grunwald B, Schoeps B, Kruger A. Recognizing the molecular multifunctionality and interactome of TIMP-1. *Trends Cell Biol* 2019;**29**:6−19.
27. Shoshan E, Braeuer RR, Kamiya T, Mobley AK, Huang L, Vasquez ME, et al. NFAT1 directly regulates IL8 and MMP3 to promote melanoma tumor growth and metastasis. *Canc Res* 2016;**76**:3145−55.
28. Van Hove I, Lemmens K, Van de Velde S, Verslegers M, Moons L. Matrix metalloproteinase-3 in the central nervous system: a look on the bright side. *J Neurochem* 2012;**123**:203−16.
29. Chu C, Liu X, Bai X, Zhao T, Wang M, Xu R, et al. MiR-519d suppresses breast cancer tumorigenesis and metastasis *via* targeting MMP3. *Int J Biol Sci* 2018;**14**:228−36.
30. Wang L, Hu L, Zhou X, Xiong Z, Zhang C, Shehada HM, et al. Author correction: exosomes secreted by human adipose mesenchymal stem cells promote scarless cutaneous repair by regulating extracellular matrix remodelling. *Sci Rep* 2018;**8**:7066.
31. Koelink PJ, Overbeek SA, Braber S, Morgan ME, Henricks PA, Abdul Roda M, et al. Collagen degradation and neutrophilic infiltration: a vicious circle in inflammatory bowel disease. *Gut* 2014;**63**:578−87.
32. Kobuch J, Cui H, Grünwald B, Saftig P, Knolle PA, Krüger A. TIMP-1 signaling *via* CD63 triggers granulopoiesis and neutrophilia in mice. *Haematologica* 2015;**100**:121590.
33. Lauhio A, Hästbacka J, Pettilä V, Tervahartiala T, Karlsson S, Varpula T, et al. Serum MMP-8, -9 and TIMP-1 in sepsis: high serum levels of MMP-8 and TIMP-1 are associated with fatal outcome in a multicentre, prospective cohort study. Hypothetical impact of tetracyclines. *Pharmacol Res* 2011;**64**:590−4.
34. Mammen MJ, Sands MF, Abou-Jaoude E, Aalinkeel R, Reynolds JL, Parikh NU, et al. Role of galectin-3 in the pathophysiology underlying allergic lung inflammation in a tissue inhibitor of metalloproteinases 1 knockout model of murine asthma. *Immunology* 2018;**153**:387−96.
35. Zou H, Wu Y, Brew K. Thermodynamic basis of selectivity in the interactions of tissue inhibitors of metalloproteinases N-domains with matrix metalloproteinases-1, -3, and -14. *J Biol Chem* 2016;**291**:11348−58.
36. Gomis-Ruth FX, Maskos K, Betz M, Bergner A, Huber R, Suzuki K, et al. Mechanism of inhibition of the human matrix metalloproteinase stromelysin-1 by TIMP-1. *Nature* 1997;**389**:77−81.
37. Wu B, Arumugam S, Gao G, Lee GI, Semenchenko V, Huang W, et al. NMR structure of tissue inhibitor of metalloproteinases-1 implicates localized induced fit in recognition of matrix metalloproteinases. *J Mol Biol* 2000;**295**:257−68.
38. Kessenbrock K, Dijkgraaf GJ, Lawson DA, Littlepage LE, Shahi P, Pieper U, et al. A role for matrix metalloproteinases in regulating mammary stem cell function *via* the Wnt signaling pathway. *Cell Stem Cell* 2013;**13**:300−13.